Physicochem. Probl. Miner. Process., 58(5), 2022, 152154

http://www.journalssystem.com/ppmp

Physicochemical Problems of Mineral Processing

ISSN 1643-1049

Multiscale water drop contact angles at selected silica surfaces

Chen Zhang [1,2], Xuming Wang [1], Lixia Li [2], Jiaqi Jin [1], Randy Polson [3], Jan D. Miller [1]

[1] Department of Materials Science & Engineering, College of Mines and Earth Sciences, University of Utah, 122 South Central Campus Drive, Room 304, Salt Lake City, UT 84112, USA

[2] School of Resources & Civil Engineering, Northeastern University, Shenyang 110819, China

[3] Utah Nanofab, 36 South Wasatch Drive, Suite 2500, University of Utah, Salt Lake City, UT 84112, USA

Corresponding author: x.wang@utah.edu (Xuming Wang)

Abstract: In this study, multiscale advancing contact angles for glycerol/water drops at silica surfaces are reported for millidrops, submicron-drops, and nanodrops. Selected silica surfaces were muscovite, silicon, and talc. The contact angles for millidrops (1–2 mm) were determined by the traditional sessile drop technique. For submicron-drops (0.1–1.0 μm), a hollow tip Atomic Force Microscope (AFM) procedure was used. The contact angles for nanodrops (~7 nm) were examined from Molecular Dynamics (MD) simulation. The results were compared to evaluate the effect of drop size on the contact angle. In the case of the hydrophobic talc surface, the 75° advancing contact angle did not vary significantly with drop size. For the hydrophilic muscovite surface, the water drop wet the surface and an advancing contact angle of about 10° was found for the millidrops and submicron-drops. However, for the MD simulated nanodrops, attachment and spreading of the ~7 nm drop created a 2D film of molecular dimensions, the contact angle of which was difficult to define and varied from 0° to 17°. Perhaps of equal interest from the MD simulation results was that the spreading of the glycerol/water nanodrop at the muscovite surface resulted in crystallographic directional transport of water molecules to the extremities of the 2D film. Such separation and segregation left the center of the film with an increased concentration of glycerol. Based on these results, the line tension, which has been found in other investigations to account for contact angle decrease with a decrease in drop size, does not seem to be a significant factor in this study.

Keywords: contact angle, atomic force microscopy, hollow tip, submicron-drop, wettability, MD simulation

1. Introduction

Contact angle at a solid surface is an important characteristic that has applications in many fields, such as in detergency, flotation, and fluid transport in porous structures (Xu et al., 2005). It is well known that the contact angle is a quantitative measure of the wettability of a solid by a liquid, which is defined geometrically as the angle formed by a liquid at the three-phase boundary (Good and Koo, 1979). At the macroscopic scale, the Young equation is a powerful tool that is widely used in wettability studies. But the shape of the attached drop is affected by gravity, and the drop may lose its spherical shape under the influence of gravity (Letellier et al., 2007), which leads to instability of the contact angle measurement. At the nanometer scale, the recent developments in Molecular Dynamics (MD) simulation, provide well-characterized surface structures with specified properties and allow one to define the nanoscale contact angle on ideal chemically homogeneous crystal surfaces (Jin et al., 2014). But, experimental verification with contact angle measurements at the nanoscale has been difficult. Experimental contact angle measurements for drop sizes between 100 - 1000 nm (submicron) remain a research challenge.

Drop size may have a significant effect on the contact angle; this has been observed and recognized experimentally at a scale above the microlevel (Drelich and Miller, 1994). However, it is a challenge to measure contact angles at the submicron level due to the evaporation of the liquid and the lack of

DOI: 10.37190/ppmp/152154

efficient procedures. Previous studies have observed droplets at the nanoscale by controlling the evaporation, such as using glycerol which has a low evaporation rate (Meister et al., 2003), decreasing the evaporation effect using rapid freezing with a cryogenic-focused ion beam (FIB), and imaging by scanning electron microscopy (SEM), the cryo-FIB/SEM) technique (Park et al., 2015). This approach has a disadvantage because it does not reflect the real shape of the drop, although images of drops at the nanoscale can be obtained. The methods used to produce submicron-drops at surfaces influence the shape of the submicron-drops. Recent research employed energy injection, such as spraying (Wang et al., 2003), but electrospray adds mechanical energy or electric energy to atomize the liquid (Jayasinghe and Edirisinghe, 2002). These methods are simple and easy to implement but may require special equipment. Other physicochemical procedures include submicron-drop preparation by emulsification (Mason et al., 2006) and condensation (Checco et al., 2006). Such experimental techniques are difficult to control which poses a potential problem to the imaging devices and hinders the practical application of these methods. Therefore, a suitable measurement method is desired for the production of submicron-drops.

Atomic force microscopy (AFM) has been widely used in imaging (Li et al., 2019) and force measurement (Nguyen et al., 2003) at the nanoscale. AFM, as a powerful imaging instrument, also can be used as a laboratory instrument with a special hollow cantilever tip, which can be used to form submicron-droplets of reproducible size by direct contact with a substrate. The transfer of liquid is controlled by the hollow tip aperture size and surface energy (Meister et al., 2004). With the use of AFM and the hollow cantilever tip, researchers have created glycerol drops (Jung and Bhushan, 2008) and other liquids with low vapor pressure (Mendez-Vilas et al., 2009). In the case of AFM-created submicron-drops, images can be obtained by the tapping mode or noncontact mode with a high-quality AFM tip (Jung and Bhushan, 2008). Drop shape can be well-described by spherical cap geometry under a small force (Ma et al., 2009). There may be accidental bridge formation between the AFM probe and the liquid surface, even the formation of a meniscus when the tip is moved slowly (Szoszkiewicz and Riedo, 2005). Lowering the temperature, changing the surface chemistry of the AFM tip, and increasing the scan rate can improve image quality. In this study, the AFM was employed as a laboratory instrument to produce hollow tip submicron-drops and to image these drops using a traditional AFM tip.

This paper presents the results of a study of the contact angles for glycerol/water submicron-drops at selected silica surfaces. The research had two principal goals. The first goal was to determine the effect of drop size on water contact angles at hydrophilic and hydrophobic surfaces; the second goal was to understand the nature of contact angles by comparison of multiscale experimental results (millidrop and submicron-drop) with MD simulation results. To obtain special AFM tips for the submicron-drop production, a silicon nitride tip was milled by dual-beam ion beam-scanning electron microscopy (FIB-SEM) to create a hollow tip about 200 nm in size. The AFM with a hollow tip and regular tip was used for the submicron-drop generation and submicron-drop imaging, respectively. The contact angle was calculated based on changes in the resonant frequency of the cantilever. This study supplements the studies of contact angles at the multiscale and gives further insight into wettability at the nanoscale.

2. Materials and methods

2.1. Materials

The samples used in this study were muscovite (V-1 grade, SPI Supplies, West Chester, PA, USA), silicon (cut from a silicon wafer), and high-quality talc crystals (Argonaut Mine, Ludlow, VT, USA).

2.2. Preparation of sample surface

To prepare atomically smooth and pure surfaces, the talc and muscovite samples were cleaved before use by removal of the top layers with scotch tape. The rms roughnesses for the silicon and the muscovite, and talc were 0.2–0.3 nm and 1.6 nm, respectively. The silicon surfaces were thoroughly cleaned and rinsed with acetone/water/methanol/water and then dried with N_2 gas before the AFM experiments.

2.3. Preparation of hollow AFM tip

The AFM probes (DNP-S10, Bruker), which consisted of a SiN tip on a SiN cantilever with a reflective gold coating on the backside, were used for milling the AFM tip. The AFM tip microfabrication diagram is shown in Fig. 1(a). The FIB/SEM was employed for milling the AFM probe. First, based on the SEM image of the tip, the geometry, including the length and width, as well as the tip specification such as the tip height, front angle, back angle, and side angle, were obtained. Then, the tip position was determined on the backside of the cantilever. Next, a hole, 5 μm in diameter, was fabricated with the FIB on the backside of the probe, centered on the tip. The hole was gradually reduced in diameter until it penetrated the tip. Finally, the tip of the probe was cut off so that the hole was exposed entirely. This preparation procedure resulted in a small hole with a diameter of 200-400 nm. Images of the hollow AFM tip with a hole are shown in Fig. 1(b).

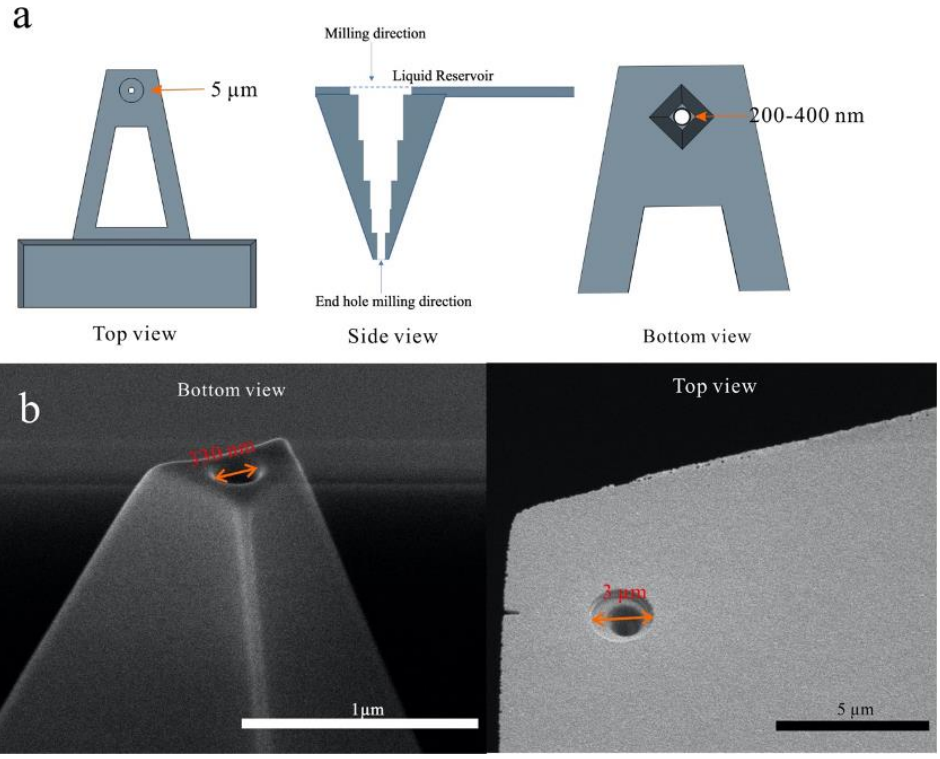

Fig. 1. Drawings of the hollow AFM tip (a); SEM images of the hollow AFM tip after preparation (b)

2.4. Submicron-drop selection and generation

When choosing the liquid to be used for the submicron-drop generation, the evaporation rate must be taken into consideration. Water is frequently used for contact angle measurements, but water has a high evaporation rate, which has made it difficult to obtain an AFM image due to the short time for image acquisition after submicron-drop deposition. Some researchers have indicated that the evaporation rates of the water droplet decreased with the addition of glycerol at the same humidity (Dashnau et al., 2006). In this regard, to overcome the problem of evaporation, a 1:9 ratio glycerol/water mixture was used for the submicron-drop deposition on the substrate surface. The effect of glycerol addition on the contact angle should be taken into consideration. Therefore, a comparison of the contact angle for water drops and the glycerol/water drops was investigated using the sessile drop technique. The results are shown in Table 1.

As shown in Table 1, the contact angles of water and glycerol are different for each of the three mineral surfaces. However, the small percentage of glycerol in the 1:9 glycerol/water mixture only has a slight effect on the contact angle, because a sufficient amount of bulk-like water exists at low glycerol concentrations (Dashnau et al., 2006). Consequently, the 1:9 glycerol/water mixture was selected as the liquid for the AFM submicron-drop generation and contact angle measurements.

Glycerol (2 cm^3) and water (18 cm^3) were mixed for 10 hours by a magnetic stirrer to prepare the

Table 1. Contact angles for water, glycerol, and a 1:9 glycerol/water mixture measured by the sessile drop technique with a drop size of about 1-2 mm

Liquid	Minerals	Contact angle (°)
Water	Muscovite	8±2
	Silicon	58±2
	Talc	79±4
Glycerol	Muscovite	22±2
	Silicon	51±2
	Talc	70±2
Glycerol/water 1:9	Muscovite	10±2
	Silicon	64±3
	Talc	75±2

glycerol/water mixture. A micropipette was used to dispense the glycerol/water mixture into the hole on the backside of the probe. As described in Section 2.3, the gold layer was removed around the hole and inside the hollow tip, to expose the SiN surface. The gold surface was much more hydrophobic than the SiN surface, which was hydrophilic, and allowed the glycerol/water mixture to flow on the SiN hydrophilic surface to reach the hollow tip. The loading area must be judiciously selected to avoid leaving the liquid along the edges since gold coated only the backside of the probe. The hollow tip showing the loading area filled with glycerol/water is shown in Fig. 2.

Fig. 2. Image of the hollow tip with the loading area partially filled with the glycerol/water mixture

Submicron-drop dispensing and spreading were conducted with the AFM (Bruker). The contact and tapping modes were used for the submicron-drop generation and cantilever resonance frequency detection, respectively. The weight of the cantilever changes with the amount of liquid loaded and dispensing leading to a change in the resonance frequency. These changes can be used to determine the weight of the submicron-drop by performing a frequency sweep of the voltage-driven oscillations using the thermal tune method (Jung and Bhushan, 2008). The main procedure for the submicron-drop formation was as follows: first, the AFM was set to the tapping mode, with the tuning of the cantilever to obtain the resonance frequency of the liquid-loaded cantilever. Then, the AFM was switched to contact mode. The scan size was set to zero nm to prevent the lateral movement of the cantilever probe from causing the liquid to discharge. The integral gain and proportional gain were set to zero so that the probe can stop immediately when it touches the surface. When the tip arrived at the sample surface, there was a transfer to ramp instead of the scan. When making a force curve, the liquid was dispensed on the surface as the tip touched the surface. Based on the differences in surface wettability, control of the ramp time was needed to obtain the right size submicron-drop. The surface wettability has

a significant effect on the drop size. On a hydrophilic surface, the glycerol/water mixture spread quickly on the surface, while on a hydrophobic surface, the drop was difficult to dispense. Finally, the AFM was set to tapping mode, using the cantilever tune to obtain the resonance frequency of the cantilever after dispensing. In this regard, the submicron-drop was prepared, and the resonance frequency was obtained before and after dispensing. A schematic diagram of the submicron-drop assembly is shown in Fig. 3.

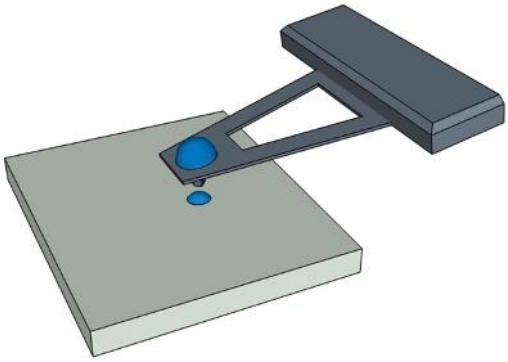

Fig. 3. The schematic diagram for submicron-drop deposition using the hollow tip AFM

2.5. Submicron-drop imaging

AFM tapping mode with a new traditional AFM probe was used for submicron-drop imaging. The resonance frequency of the cantilever was calibrated before imaging. The wettability of the tip may influence the imaging, so the cantilever amplitude was set as necessary to ensure that the tip touched the submicron-drop with minimal force and good image quality. A faster scan rate was adopted to minimize the influence of evaporation on the shape of the submicron-drop, and the resolution was set to 512 lines. NanoScope Analysis 1.8 was employed for the post-processing of the image.

2.6. Molecular Dynamics (MD) simulation of glycerol/water nanodrops

The Amber software package was used to conduct the MD simulated glycerol/water drops in this study (Pearlman et al., 1995). Glycerol/water drops with the molecular ratios of 1:9 and 1:3 were prepared using SPC/E for the water model and OPLS for the glycerol model (Mark and Nilsson, 2001; Kaminski et al., 2001). The drop diameter was about 7 nm. The crystal structures of muscovite and talc were from the American Mineralogist Crystal Structure Database, as determined by XRD (Downs and Hall-Wallace, 2003). The MD simulations were done in the NVT ensemble with atoms of the silica mineral in fixed positions. A constant number, volume, and temperature condition was used for an MD simulation of 2 ns, to allow the drop attachment and spreading at the selected silica surfaces. The simulated drop was projected to the X-O-Z and Y-O-Z planes to determine the contact angles. The averaged values were reported as the contact angle of the MD simulated ~7 nm glycerol/water drops.

3. Results and discussion

3.1. Results

The submicron-drops were generated on the muscovite, silicon, and talc surfaces, and the AFM images of the submicron-drops are shown in Fig. 4. As shown in Fig. 4 that the submicron-drop was successfully created by the hollow tip and imaged by the AFM using the tapping mode. Comparing the drop images on the surfaces of different wettability, the submicron-drop on muscovite presented a high-quality round shape, which is because the contact angle for muscovite was the smallest, which means after spreading, the drop body was relatively flat on the smooth muscovite surface (rms = 0.2-0.3 nm). The drop size varied from 250 nm to 1.5 μm at the different surfaces as shown in Fig. 4. The wetting features were determined by the surface polarity and were challenging to control. The liquid was quickly sucked from the hollow tip to the surface when close to the hydrophilic surface (such as muscovite), while at the hydrophobic surfaces, the submicron-drops were challenging to generate and attach, as expected.

In the case of the hydrophobic surface, a greater volume of the liquid was needed to detach the drop from the tip

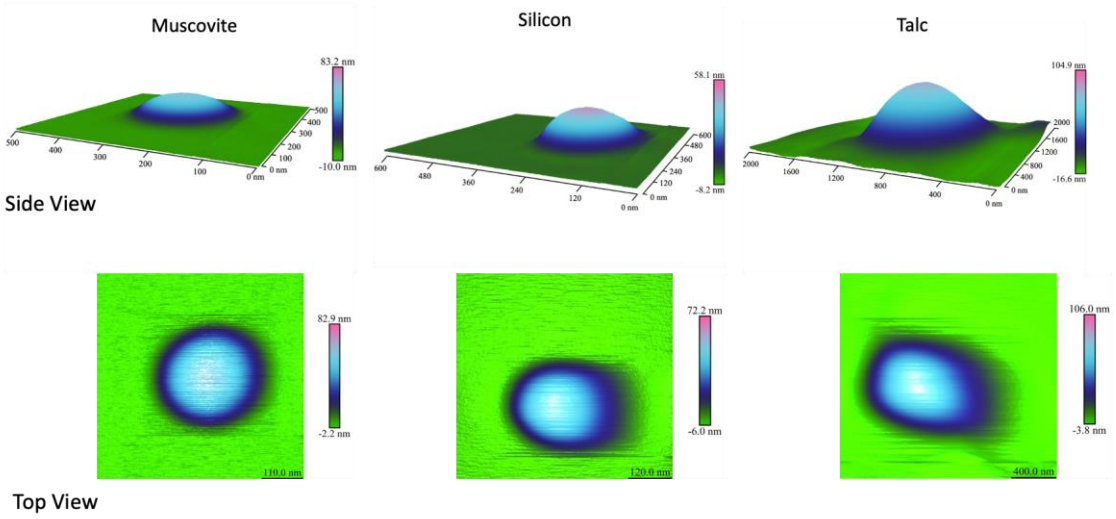

Fig. 4. Side view and corresponding top view of the 3D AFM images of 1:9 glycerol/water submicron-drops on muscovite, silicon, and talc surfaces

Some researchers use a section of the drop from the images to measure the contact angle, but this method was significantly affected by the unit length of the X and Z axis, which resulted in inconsistent results. Calculation of the contact angle base on the submicron-drop volume provides a better solution. According to the shift of the cantilever resonance frequency before and after deposition, the volume of the liquid deposited on the surface can be estimated by Eq. 1 (Jung and Bhushan, 2008):

$$w_C = \frac{1}{2\pi}\sqrt{\frac{k}{m_C}} \tag{1}$$

Eq. 1 shows the relationship between the resonance frequency and the mass of the cantilever, where w_C is the resonance frequency of the cantilever; k is the spring constant of the cantilever; m_C is the mass of the cantilever.

The resonance frequency will be affected by the mass of the cantilever and the submicron-drop after the liquid is loaded onto the cantilever. Therefore, the resonance frequency of the loaded cantilever (w_L) can be found in Eq. 2 (Jung and Bhushan, 2008):

$$w_L = \frac{1}{2\pi}\sqrt{\frac{k}{m_C+m_L}} \tag{2}$$

Where m_L is the mass of the liquid loaded on the hollow tip. The resonance frequency after the submicron-drop is deposited on the surface(w_D) is given by Eq. 3:

$$w_D = \frac{1}{2\pi}\sqrt{\frac{k}{m_C+m_L-m_D}} \tag{3}$$

Where m_D is the mass of the submicron-drop. Due to the glycerol/water mixture, the mass evaporated from the cantilever during the process was negligible. Therefore, the mass of the submicron-drop can be found in Eq. 4:

$$m_D = m_C + m_L - \frac{1}{(2\pi)^2 w_D^2} \tag{4}$$

The density of the liquid mixture (ρ) is 1.026 g/cm^3. Combining Eqs. 1 and 4, the volume of the submicron-drop deposited on the surface can be obtained by Eq. 5:

$$V = \frac{1}{\rho}\left[\frac{k}{(2\pi)^2}\left(\frac{1}{w_L^2}-\frac{1}{w_D^2}\right)\right] \tag{5}$$

As shown in Fig. 5, r is the radius of the submicron-drop with a contact diameter d of the droplet cap at the surface. The thickness of the droplet, h, and the volume of the submicron-drop, V, is given in Eq. 6 (Jung and Bhushan, 2008):

$$V = \frac{1}{3}\pi h^2(3r - h) \tag{6}$$

From Fig. 5, r can be found in Eq. 7:

$$r = \frac{d}{2\sin\theta} \tag{7}$$

Combining Eqs. 6 and 7, the equation for the contact angle, θ, of each submicron-drop can be calculated from Eq. 8:

$$\theta = \sin^{-1}\left(\frac{3d}{2(\frac{3V}{\pi h^2}+h)}\right) \tag{8}$$

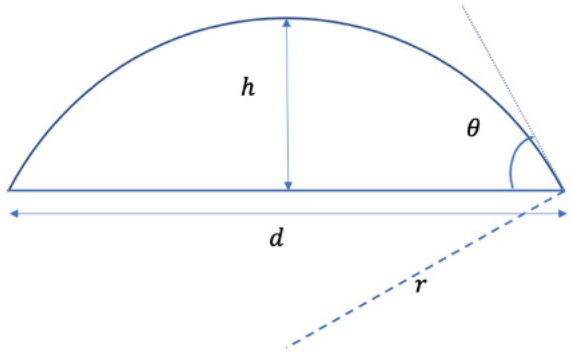

Fig. 5. Submicron-drop generated at the surface with a contact angle θ, and thickness, h. The contact diameter between the droplet and the surface is d and the radius of the curvature of the droplet is r

To obtain the parameters for the submicron-drop calculation, the resonance frequency was recorded during the experiment, and the section was obtained from the morphological data. In order to reduce the error, a section was made every 60° on the AFM image of the submicron-drop, and then the average value was calculated for each parameter. Figure 6 shows the appearance of the submicron-drop, and the corresponding parameters are presented in Table 2.

Figure 6 depicts the 3D submicron-drops on the muscovite, silicon, and talc surfaces, and the corresponding section images. The distance and height data were obtained from the section images. Based on Eqs. 5 and 8, the contact angles of the submicron-drops were obtained and are shown in Table 2. The contact angles of muscovite, silicon, and talc were 9°, 53°, and 75°, respectively.

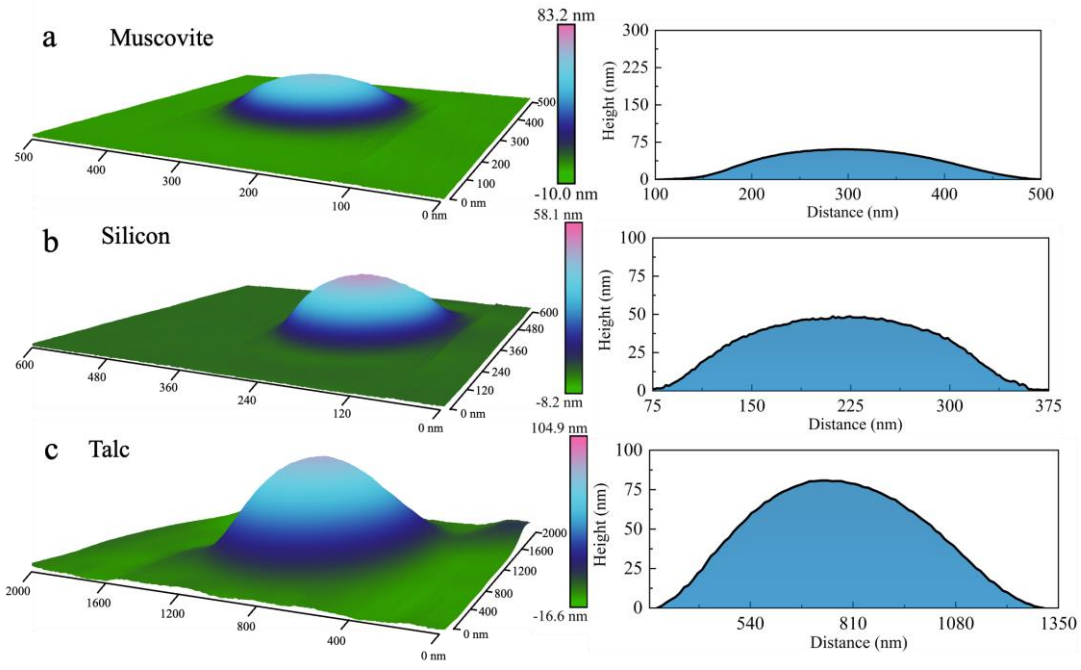

Fig. 6. Side view of 3D AFM images and selected section images of 1:9 glycerol/water submicron-drops on muscovite (a), silicon (b), and talc (c) surfaces

Table 2. Contact angle data for the submicron-drops from Fig. 6

Minerals	Resonance Frequency		Shape data*		Contact angle (°)
	Loaded (kHz)	Deposited (kHz)	Average Distance (nm)	Average Height (nm)	
Muscovite	59.0492	59.1127	304	43	9
Silicon	59.2107	59.2274	331	48	53
Talc	59.1910	59.2822	726	84	75

* all lengths were obtained by averaging the measurements every 60°.

The MD simulated ~7 nm glycerol/water nanodrops (ratio of 1:3) at the muscovite (001) and talc (001) surfaces are shown in Figs. 7(a) and (b), respectively. The MD simulated glycerol/water nanodrop spread at the muscovite (001) surface, and the contact angle, which varied from 0° to 17°, was difficult to define. In contrast, the MD simulated glycerol/water nanodrop formed a hemispherical shape at the talc surface with a 75° contact angle (Fig. 7b). The ~7 nm glycerol/water nanodrops with the ratio of 1:9 at the selected silica surfaces were also simulated by MD, and the same results were found.

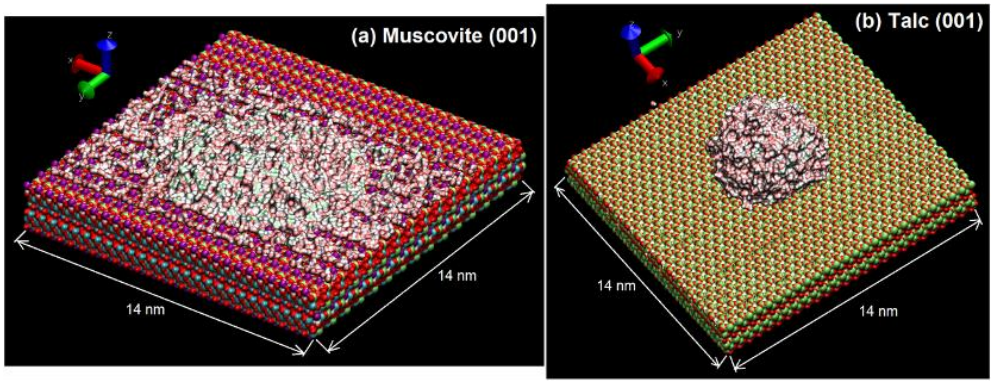

Fig. 7. Snapshot of MD simulated ~7 nm glycerol/water drops (ratio of 1:3) at the muscovite (001) surface (a) and talc (001) surface (b)

3.2. Discussion

In order to evaluate the multiscale aspect of wetting, a comparison of results from traditional sessile millidrops, AFM submicron-drops, and MD simulated nanodrops is listed in Table 3.

Many studies have discussed the effect of drop size on contact angle and wetting. Regarding the surface properties of the samples, some researchers (Wang et al., 2002) pointed out that the organic contaminants on specimen surfaces might give rise to a higher surface hydrophobicity, and their distribution at the nanoscale may differ from that at the milliscale. Checco et al. (2003) proposed that the surface heterogeneities may be responsible for the observed decrease in contact angle with a decrease in drop size. Drelich and Miller (1994) investigated the effect of drop size on advancing and receding contact angles for rough solid surfaces by sessile drop and captive bubble techniques. The results indicated that the roughness causes contortions in the shape of the three-phase contact line, which may help to explain the drop size dependence of the contact angle.

Table 3. Comparison of advancing contact angles from millidrops, AFM submicron-drops, and MD nanodrops

Liquid Glycerol/water (1:9 by vol.)	Mineral	Contact angles (°)		
		Millidrops Goniometer (1-2 mm)	Submicron-drops AFM (100-1000 nm)	Nanodrops MD Simulation (~7 nm)
	Muscovite	10±2	9	0-17
	Silicon	64±3	53	
	Talc	75±2	75	75

The physical properties of specimen surfaces may play an important role in explaining the variation of contact angle with drop size. However, through holistic treatment, the effects become irrelevant. In view of the impact of molecular and interfacial forces on the contact angle, the line tension, and the excess free energy per unit of the three-phase contact line, has been considered to explain the experimental results (Weijs et al., 2011). As the size of a droplet decreases, the relative proportion of molecules in the vicinity of the contact line increases, so the effect of line tension becomes more important. In the presence of finite line tension, the contact angle of a liquid droplet depends on its size. Therefore, when the drop size decreases and the effect of gravity decreases, line tension may contribute to the change of contact angle at the nanoscale (Drelich and Miller, 1994).

Based on consideration of line tension, the contact angle at the nanoscale might be expected to be smaller than that at the milliscale. As shown in Table 3, there is no contact angle change for the hydrophobic talc surface. The contact angle is a constant 75° at all drop sizes; millidrops, submicron-drops, and nanodrops. In contrast, at the hydrophilic muscovite surface the contact angle is about 10° for millidrops and submicron-drops but is difficult to determine for the MD nanodrop because the drop shape is not so well defined, and might better be considered as a 2-dimensional film which wets the muscovite surface.

In the case of the MD nanodrop, the muscovite surface may be considered to be completely wet the surface (0° contact angle), or perhaps be as large as 17° depending on the analysis. The difficulty is in defining the boundary of the nanodrop, or 2D film, with a maximum thickness of 1.2 nm at the center, a thickness probably corresponding to no more than two glycerol molecules. Perhaps of equal interest is the observation from MD simulation that the glycerol/water (1:3) drop is fractionated during spreading after attachment. It seems that water molecules migrate directionally to the extremities of the film following the K^+ of the muscovite crystallographic structure. The glycerol molecules tend to remain behind with some water molecules in a more concentrated mixture as seen in Fig. 8.

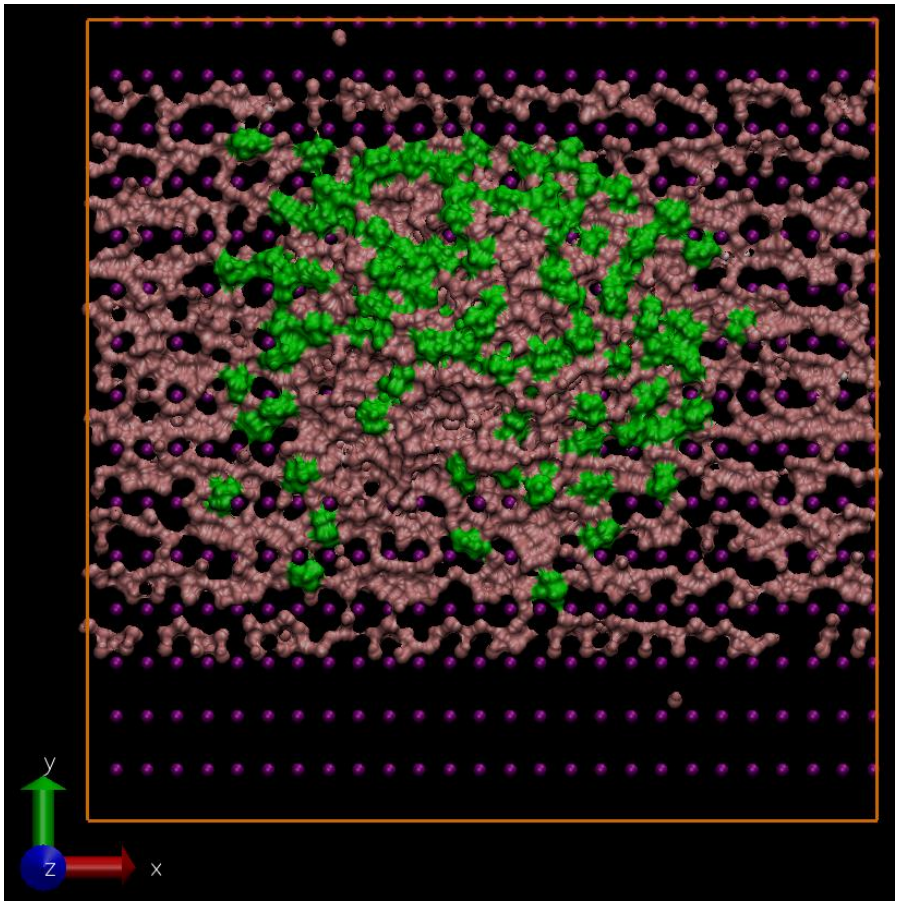

Fig. 8. Top view of an MD simulated ~7 nm glycerol/water nanodrop (glycerol/water = 1:3) at the muscovite (001) surface. Color codes: purple, potassium cations at muscovite (001) surface; pink, water molecules; green, glycerol molecules

4. Summary and conclusions

The hollow tip AFM procedure to measure advancing contact angles of submicron-drops provides a way to obtain contact angles at the submicron scale and allows comparison with traditional milliscale measurements. In this way, a better understanding of multiscale wettability is possible. The contact angles for glycerol/water (1:9) submicron-drops were determined for muscovite, silicon, and talc surfaces. The images of submicron-drops were obtained with the AFM tapping mode. Based on the change of resonance frequency and the submicron-drop topographic data from the AFM images, the contact angles of submicron-drops were calculated. The submicron-drop contact angles were the same as those measured at the milliscale for muscovite and talc, but the contact angles differed by 10° for the silicon surface. The line tension, which may account for contact angle decrease with a decrease in drop size, does not seem to be very significant in the case of submicron and nanometer drops at the muscovite and talc surfaces. Line tension may help to explain the small difference in contact angle, which can be generally neglected at the milliscale. The results indicate that the advancing contact angle is independent of drop size for these surfaces, and suggest that the line tension is not significant. In addition to the independence of contact angle on drop size, it should be noted that the ~7 nm MD nanodrop wets the hydrophilic muscovite surface creating a 2D film in which the water molecules spread directionally and separate from the glycerol molecules. Consequently, the contact angle becomes difficult to define due to molecular segregation. These insights contribute to an improved understanding of the multiscale effect of drop size on contact angle and should be useful in many areas of technology including fluid transport in porous structures, and flotation separations associated with the processing of mineral resources.

Acknowledgments

The authors thank Ms. Dorrie Spurlock for her assistance with the preparation of this paper. The authors acknowledge funding from the Joint Fund (Key program U2067201) for Nuclear Technology Innovation sponsored by the National Natural Science Foundation of China and the China National Nuclear Corporation and Fundamental Research Funds for the Central Universities (N2001013) to support Chen Zhang's research at the University of Utah.

This research was supported as part of the Multi-Scale Fluid-Solid Interactions in Architected and Natural Materials (MUSE), an Energy Frontier Research Center funded by the US Department of Energy, Office of Science, Basic Energy Sciences program, under award DE-SC0019285.

References

CHECCO, A., GUENOUN, P., DAILLANT, J., 2003. *Nonlinear dependence of the contact angle of nanodroplets on contact line curvature.* Physical Review Letters, 91, 186101.

CHECCO, A., SCHOLLMEYER, H., DAILLANT, J., GUENOUN, P., BOUKHERROUB, R., 2006. *Nanoscale wettability of self-assembled monolayers investigated by noncontact atomic force microscopy.* Langmuir, 22, 116-126.

DASHNAU, J.L., NUCCI, N.V., SHARP, K.A., VANDERKOOI, J.M., 2006. *Hydrogen bonding and the cryoprotective properties of glycerol/water mixtures.* The Journal of Physical Chemistry B, 110, 13670-13677.

DOWNS, R.T., HALL-WALLACE, M., 2003. *The American Mineralogist crystal structure database.* American Mineralogist, 88 (1), 247-250.

DRELICH, J., MILLER, J.D., 1994. *The effect of solid surface heterogeneity and roughness on the contact angle/drop (bubble) size relationship.* Journal of Colloid and Interface Science, 164, 252-259.

GOOD, R.J., KOO, M., 1979. *The effect of drop size on contact angle.* Journal of Colloid and Interface Science, 71, 283-292.

JAYASINGHE, S., EDIRISINGHE, M., 2002. *Effect of viscosity on the size of relics produced by electrostatic atomization.* Journal of Aerosol Science, 33, 1379-1388.

JIN, J., MILLER, J.D., DANG, L.X., 2014. *Molecular dynamics simulation and analysis of interfacial water at selected sulfide mineral surfaces under anaerobic conditions.* International Journal of Mineral Processing, 128, 55-67.

JUNG, Y.C., BHUSHAN, B., 2008. *Technique to measure contact angle of micro/nanodroplets using atomic force microscopy.* Journal of Vacuum Science & Technology A: Vacuum, Surfaces, and Films, 26, 777-782.

KAMINSKI, G.A., FRIESNER, R.A., TIRADO-RIVES, J., JORGENSEN, W.L., 2001. *Evaluation and reparametrization of the OPLS-AA force field for proteins via comparison with accurate quantum chemical calculations on peptides.* The Journal of Physical Chemistry B, 105(28), 6474-6487.

LETELLIER, P., MAYAFFRE, A., TURMINE, M., 2007. *Drop size effect on contact angle explained by nonextensive thermodynamics. Young's equation revisited.* Journal of Colloid and Interface Science, 314, 604-614.

LI, L., ZHANG, C., YUAN, Z., XU, X., SONG, Z., 2019. *AFM and DFT study of depression of hematite in oleate-starch-hematite flotation system.* Applied Surface Science, 480, 749-758.

MA, J., JING, G., CHEN, S., YU, D., 2009. *Contact angle of glycerol nanodroplets under van der Waals force*. Journal of Physical Chemistry C, 113, 16169–16173.

MARK, P., NILSSON, L., 2001. *Structure and dynamics of the TIP3P, SPC, and SPC/E water models at 298 K.* The Journal of Physical Chemistry A, 105(43), 9954-9960.

MASON, T.G., WILKING, J.N., MELESON, K., CHANG, C.B., GRAVES, S.M., 2006. *Nanoemulsions: Formation, structure, and physical properties.* Journal of Physics: Condensed Matter, 18, R635.

ME´NDEZ-VILAS, A., BELE´N JO´DAR-REYES, A., MARI´A LUISA GONZA´LEZ-MARTI´N. 2009. *Ultrasmall liquid droplets on solid surfaces: Production, imaging, and relevance for current wetting research.* Small, 5(12), 1366–1390.

MEISTER, A., JENEY, S., LILEY, M., AKIYAMA, T., STAUFER, U., DE ROOIJ, N., HEINZELMANN, H., 2003. *Nanoscale dispensing of liquids through cantilevered probes.* Microelectronic Engineering, 67, 644-650.

MEISTER, A., LILEY, M., BRUGGER, J., PUGIN, R., HEINZELMANN, H., 2004. *Nanodispenser for attoliter volume deposition using atomic force microscopy probes modified by focused-ion-beam milling.* Applied Physics Letters, 85, 6260-6262.

NGUYEN, A.V., NALASKOWSKI, J., MILLER, J.D., BUTT, H.-J., 2003. *Attraction between hydrophobic surfaces studied by atomic force microscopy.* International Journal of Mineral Processing, 72, 215-225.

PARK, J., HAN, H.-S., KIM, Y.-C., AHN, J.-P., OK, M.-R., LEE, K.E., LEE, J.-W., CHA, P.-R., SEOK, H.-K., JEON, H., 2015. *Direct and accurate measurement of size dependent wetting behaviors for sessile water droplets.* Scientific Reports, 5, 1-12.

PEARLMAN, D.A., CASE, D.A., CALDWELL, J.W., ROSS, W.S., CHEATHAM III, T.E., DEBOLT, S., FERGUSON, D., SEIBEL, G., KOLLMAN, P., 1995. *AMBER, a package of computer programs for applying molecular mechanics, normal mode analysis, molecular dynamics and free energy calculations to simulate the structural and energetic properties of molecules.* Computer Physics Communications, 91(1-3), 1-41.

SZOSZKIEWICZ, R., RIEDO, E., 2005. *Nucleation time of nanoscale water bridges.* Physical Review Letters, 95, 135502.

WANG, R., KIDO, M., MORIHIRO, N., 2003. *An XPS and atomic force microscopy study of the micro-wetting behavior of water on pure chromium.* Materials Transactions, 44, 389-395.

WANG, R., TAKEDA, M., KIDO, M., 2002. *Micro pure water wettability evaluation with an AC no-contact mode of atomic force microscope.* Materials Letters, 54, 140-144.

WEIJS, J.H., MARCHAND, A., ANDREOTTI, B., LOHSE, D., Snoeijer, J.H., 2011. *Origin of line tension for a Lennard-Jones nanodroplet.* Physics of Fluids, 23, 022001.

XU, L., ZHANG, W.W., NAGEL, S.R., 2005. *Drop splashing on a dry smooth surface.* Physical Review Letters, 94, 184505.